Increased Polarization Caused by Films Covering Hyperfiltration Membranes

JOHN D. SHEPPARD and DAVID G. THOMAS

Oak Ridge National Laboratory, Oak Ridge, Tennessee 37830

Membrane fouling is a problem which may be encountered with hyperfiltration systems used for desalting natural waters. Although plant feeds are generally prefiltered to remove particulate matter (*1* to *4*), nonfiltered material and plant corrosion products may be deposited on the membrane surface in sufficient quantities to affect plant performance. In some cases, fouling with pretreated feeds (*3*) has been sufficiently severe to require scrubbing by passage of an oversize polyurethane sponge ball through the tubes (*4*).

We have reported studies (*5*) in which fouling of cellulose acetate membranes by unfiltered lake water feed was arrested by operation at high axial velocities. Whereas operation in at least well-developed turbulent flow ($N_{Re} > 10^4$) is necessary to control concentration polarization, much higher velocities were required to control fouling.

Effects of fouling on plant performance can be observed in decreased production rate (flux decline) and in decreased product water quality (rejection decline). Fouling studies are complicated by the fact that these two effects are not necessarily coupled in the manner that flux and rejection of unfouled membranes are coupled. Other causes of reduced plant performance, such as membrane hydrolysis (*6*) and mechanical deformation (compaction), may also complicate fouling studies. For example, both fouling and hydrolysis reduce product water quality; however fouling decreases production rate and hydrolysis (*6*) tends to increase production rate.

The objective of this study is to predict quantitatively the rejection of hyperfiltration membranes which are covered by uniform layers of fouling material. In order to relate reduced product water quality quantitatively to the characteristics of fouling layers, we used uniform, permeable plastic films as a substitute for fouling layers.

BACKGROUND

Important performance characteristics of hyperfiltration systems are the water transmission rate (flux) through the membrane and the rejection of salt by the membrane. The transmission rate is reasonably approximated (*7*) by

$$J = \mathcal{P}\,(\Delta P - \Delta\pi) \tag{1}$$

The osmotic pressure (*8*) is nearly a linear function of salt concentration at constant temperature

$$\pi = \varphi\,\nu\,\mathcal{R}T\,m \tag{2}$$

The intrinsic rejection of the membrane is defined as

$$R \equiv 1 - \frac{c_\omega}{c_\alpha} \tag{3}$$

We also define the observed rejection

$$R_{\text{obs}} \equiv 1 - \frac{c_\omega}{c_t} \tag{4}$$

The difference in observed and intrinsic rejections is due to salt buildup adjacent to the membrane, known as concentration polarization

$$\psi \equiv \frac{c_\alpha}{c_t} - 1 \tag{5}$$

Even if the intrinsic rejection of a membrane is high ($R \simeq 1$), the quality of the product stream may be poor because of concentration polarization. Product water quality can be improved by increasing mass transfer between the membrane surface and the bulk feed stream circulating past the membrane. Operation of a hyperfiltration system in fully developed turbulent flow is a common means of attaining high mass transfer and reducing concentration polarization.

Mass transfer in the turbulent boundary layer adjacent to a perfectly rejecting membrane was treated by Sherwood et al. (*9*) using a film theory model. Johnson et al. (*7*) and Brian (*10*) have extended the analysis to give concentration polarization of imperfectly rejecting membranes. In terms of salt rejection

$$\ln\frac{1-R_{\text{obs}}}{R_{\text{obs}}} = \ln\left(\frac{1-R}{R}\right) + \frac{kv}{u}\,N_{Re}^{1/4}\,N_{Sc}^{2/3} \tag{6}$$

Based on Equation (6), the intrinsic rejection may be determined by plotting $\ln[(1 - R_{\text{obs}})/R_{\text{obs}}]$ versus $v/u^{3/4}$ and extrapolating the data to infinite circulation velocity. This technique has been used in several experimental hyperfiltration studies (*5*, *12* to *16*).

An effect, not included explicitly in Equations (1) through (6), is the variation in intrinsic rejection with transmission rate. Johnson et al. (*7*) have presented a relationship among intrinsic rejection, a membrane flow parameter σ, a solvent-solute coupling coefficient β, and a distribution coefficient D^*:

$$\frac{1-R}{R} = \left[\frac{e^{\beta\sigma}}{e^{\beta\sigma}-1}\right]\left[\frac{\beta D^*}{1-\beta D^*}\right] \tag{7}$$

The flow parameter is

$$\sigma = \frac{v\,l}{\mathcal{D}_2^*} \tag{8}$$

For small values of $\beta\sigma$

$$\frac{1-R}{R} \propto \frac{1}{\beta\sigma} \propto \frac{1}{v} \tag{9}$$

Since the range of values of β is $0 < \beta < 1$ (*7*), if σ is small, then Equation (9) should be valid. Furthermore, if β is small, Equation (9) should remain valid for greater values of σ (or v).

Equation (9) has been verified experimentally for cellu-

Correspondence concerning this article should be addressed to Dr. David G. Thomas, Reactor Division, Oak Ridge National Laboratory, P.O. Box Y, Oak Ridge, Tennessee 37839.

lose acetate (*5, 14* to *17*); this effect must be taken into account in fouling studies since fouling may significantly reduce the membrane transmission rate.

EFFECT OF A UNIFORM, PERMEABLE NONREJECTING LAYER

Based on the above discussion, a permeable film may have major effects on membrane performance: (1) an added resistance to flow which reduces the flux through the membrane, and consequently, reduces the intrinsic rejection [Equation (9)]; and (2) an added resistance to mass transfer in the boundary layer which increases concentration polarization, resulting in reduced observed rejection and increased osmotic pressure. These effects are similar to those caused by the spongy membrane surface described briefly by Brian (*11*).

Consider an imperfectly rejecting membrane ($R < 1$), on the high pressure side of which is a uniform layer of material with no salt rejection capability (Figure 1). The steady state transport of salt in the system is given by

$$v\, c_\omega = \mathcal{D}\frac{dc}{dy} + v\, c \qquad (10)$$

where y is taken as zero at the membrane-film interface. Equation (10) must be integrated from the membrane surface to the feed stream taking into account the difference in diffusivities in the permeable film and the feed stream to give the total concentration polarization, that is

$$\int_{c_\alpha}^{c_t} \frac{-dc}{c-(1-R)c_\alpha} = \int_0^{\delta_g} \frac{v\,dy}{\mathcal{D}_g} + \int_{\delta_g}^{\delta t} \frac{v\,dy}{\mathcal{D}} \qquad (11)$$

Integration of Equation (11) across the two resistances utilizing the film theory model for the feed stream portion (*7, 9, 11*) and assumption that the diffusion coefficient of salt in the permeable, nonrejecting layer is constant (which

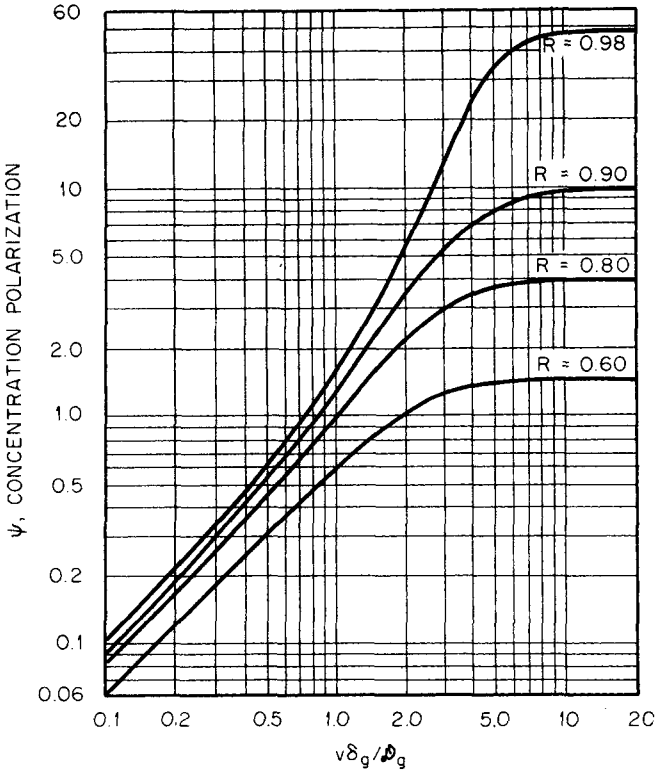

Fig. 2. Concentration polarization in a permeable film on the high pressure side of a hyperfiltration membrane as a function of $v\,\delta_g/\mathcal{D}_g$ and intrinsic rejection R.

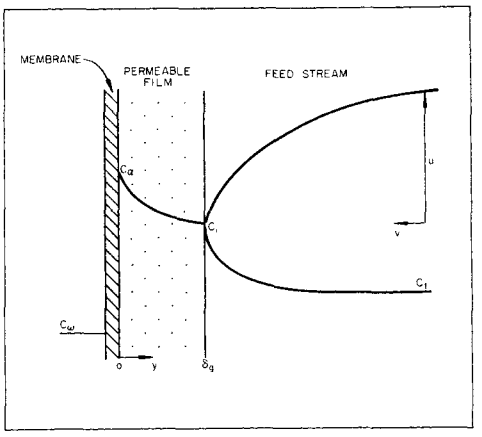

Fig. 1. Schematic diagram of hyperfiltration process with a permeable film covering the high pressure side of a membrane.

implies uniform porosity and negligible variation in diffusivity with the concentration in a layer at a given time) gives

$$\ln\left[\frac{1-R_{obs}}{R_{obs}} \Big/ \frac{1-R}{R}\right] = \frac{v\delta_{BL}}{\mathcal{D}} + \frac{v\delta_g}{\mathcal{D}_g} \qquad (12)$$

where concentrations are given in terms of R and R_{obs} [Equations (3) and (4)]. Incorporation of the mass momentum transfer analogy used in deriving Equation (6) into Equation (12) and rearrangement give

$$\ln\left[\frac{1-R_{obs}}{R_{obs}}\right] = \frac{kv}{u} N_{Re}^{1/4} N_{Sc}^{2/3} + \frac{v\delta_g}{\mathcal{D}_g} + \ln\left[\frac{1-R}{R}\right] \qquad (13)$$

If there is no nonrejecting layer ($\delta_g = 0$), Equation (13) reduces to Equation (6). With infinite circulation velocity, Equations (12) and (13) reduce to

$$\ln\left[\frac{1-R_{obs}}{R_{obs}} \Big/ \frac{1-R}{R}\right]_{u=\infty} = \frac{v\delta_g}{\mathcal{D}_g} \qquad (14)$$

from which the concentration polarization due to the permeable film can be determined.

Limiting values of concentration polarization due to permeable layers covering a membrane can be determined by rewriting Equation (14) in terms of concentration polarization. The observed and intrinsic rejections may be related to concentration polarization by substituting Equations (3) and (4) into Equation (5):

$$\psi = \frac{1-R_{obs}}{1-R} - 1 \qquad (15)$$

Combining Equations (14) and (15) gives the polarization due to the nonrejecting layer:

$$\psi_g = \frac{R\,[1-\exp(-v\,\delta_g/\mathcal{D}_g)]}{1-R\,[1-\exp(-v\,\delta_g/\mathcal{D}_g)]} \qquad (16)$$

For $v\,\delta_g/\mathcal{D}_g \ll 1$

$$\exp(-v\,\delta_g/\mathcal{D}_g) \simeq 1 - v\,\delta_g/\mathcal{D}_g \qquad (17)$$

and Equation (16) reduces to

$$\psi_g = R\,v\,\delta_g/\mathcal{D}_g \qquad (18)$$

Also, as

$$v\,\delta_g/\mathcal{D}_g \to +\infty \qquad (19)$$

$$\psi_g \to R/1-R \qquad (20)$$

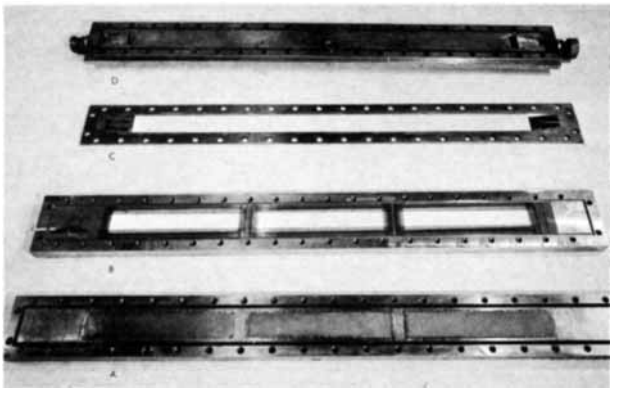

Fig. 3. Rectangular channel test section. (*a*) Permeable wall. (*b*) Permeable wall with membranes. (*c*) Spacing plate defining ¼-in. × 2½-in. flow channel. (*d*) Impermeable wall with flow inlet and exit.

which is the maximum contribution to concentration polarization by nonrejecting layers adjacent to a membrane with intrinsic rejection R. [For laminar flow past a clean membrane, the maximum concentration polarization is also $R/(1-R)$ (7).]

Concentration polarization in the gel layer ψ_g, calculated from Equation (16), is shown in Figure 2 as a function of $v\ \delta_g/\mathcal{D}_g$ with intrinsic rejection R as a parameter. The asymptotic value of ψ_g is essentially obtained at $v\ \delta_g/\mathcal{D}_g = 10$.

It must be emphasized that Equation (16) gives only the concentration polarization due to the permeable layer. If the salt concentration at the film-feed stream interface is c_i, total concentration polarization for finite axial velocities is given by

$$\psi = \frac{c_\alpha}{c_i}\,\frac{c_i}{c_t} - 1 \qquad (21)$$

or

$$\psi = [\psi_g + 1]\,[\psi_{BL} + 1] - 1 \qquad (22)$$

where ψ_g and ψ_{BL} are the concentration polarization in the permeable film and boundary layers, respectively.

EXPERIMENTAL EQUIPMENT

Our experimental study utilized a high pressure, 50-liter hyperfiltration loop, important features of which were a pressurizing pump, a circulating pump, and a rectangular channel test section. The pressurizing pump was a variable-flow, variable-pressure feeder pump with capacity up to several thousand gallons per day and pressure to 2,000 lb/sq.in. gauge. A 50 gal./min. canned rotor centrifugal pump provided a velocity range of 0.1 to 24 ft./sec. in the test section. Flow rates were determined by calibrated Venturi meters.

The stainless steel test section, Figure 3, was of rectangular cross section, ¼ in. × 2½ in., and had three porous sections on one wall, allowing three membranes, 2 in. wide × 12 in. long, to be tested independently at the same feed condition. The permeable wall consisted of porous stainless steel plate (~35 μ mean pore size) mounted flush to the inside channel wall and backed with perforated (0.125-in. holes) plates. The inlet to the test section was designed to reduce flow disturbances.

Holdup and mixing tanks in the low pressure portion of the loop add 50 liters vol. to the system requiring 100 liters of feed solution for operation. A letdown valve allowed continuous mixing of the high and low pressure feed streams and provided a feed sample for analysis. Feed solutions were prepared by adding reagent grade sodium chloride to demineralized water to give ~0.1 M NaCl. Feed and product concentrations were determined by amperometric titration of the chloride ion using a Buchler-Cotlove Chloridometer; the accuracy was ±0.5%.

The hyperfiltration membranes used were commercial cellulose acetate membranes, either Aerojet-General 6% permeation membranes or Eastman RO-97 membranes. For both the Aerojet-General and Eastman membranes, a single stock of material was used. The rejection-transmission rate relationship [Equation (7)] was determined primarily by pressure excursions at 24 ft./sec. axial velocity. It has been shown (*5, 14*) that at 24 ft./sec. the observed and intrinsic rejections differed only slightly and the error in plotting $(1 - R_{obs})/R_{obs}$ instead of $(1-R)/R$ was less than 10%. The variation in rejection with flux for the membranes is given in Figure 4. The data are in agreement with Equation (9), which predicts a −1 slope on the log-log plot.

The cellulose acetate membranes were sealed to the test section with pressure-sensitive, polyester silicone tape. The membranes were then covered with porous, nonrejecting films which were also sealed to the test section with tape. Two types of nonrejecting films were used: Eastman cellulose acetate (HT-OO), which had not been heat treated, and Millipore

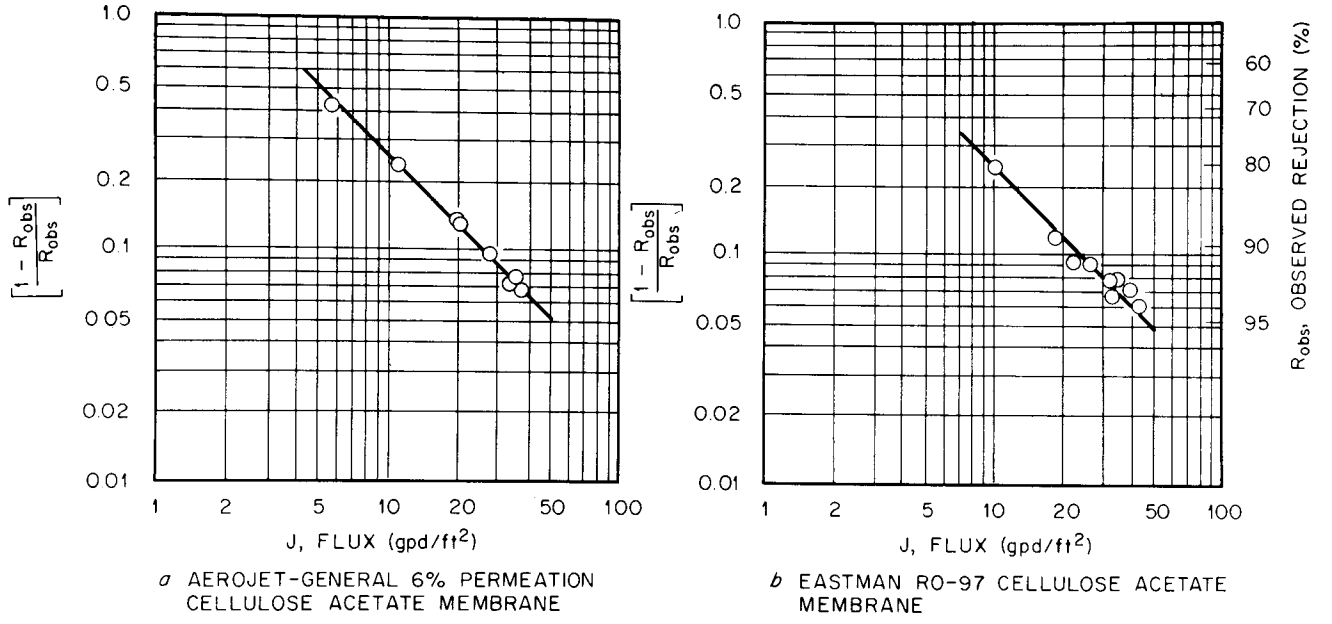

a AEROJET-GENERAL 6% PERMEATION CELLULOSE ACETATE MEMBRANE

b EASTMAN RO-97 CELLULOSE ACETATE MEMBRANE

Fig. 4. Variation in rejection with flux through cellulose acetate membranes (0.1 M NaCl in demineralized water; 30°C).

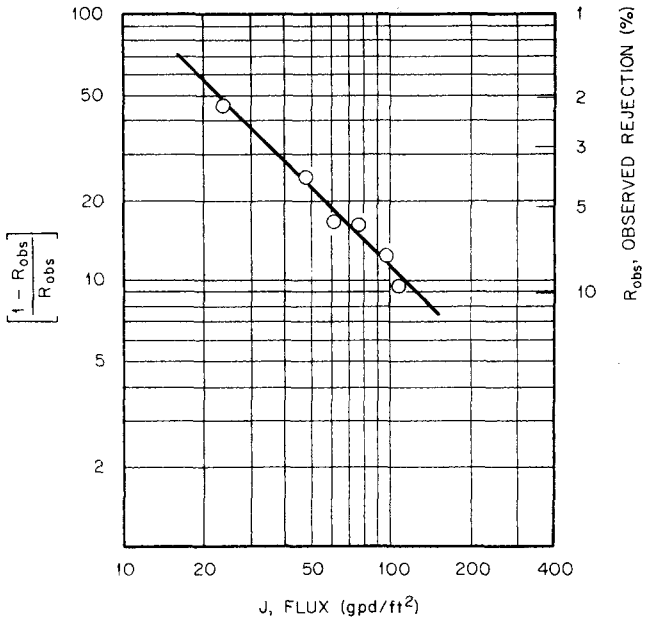

Fig. 5. Variation in rejection with flux through Eastman HT-OO nonheat-treated cellulose acetate film (0.1 M NaCl in demineralized water; 24 ft./sec. axial velocity).

filter (nominal 0.1 μ pore size). These films were much more permeable to solvent flow than the rejecting membrane; thus even with two layers of film covering the membrane, the flux-effective pressure relationship was that given by Equation (1). This is in contrast to the gel-layer effect described by Michaels (*27*) in which there is appreciable hydrostatic pressure loss across the gel layer and the flux is virtually independent of applied pressure. In both cases, however, the equations developed in this paper should be applicable.

To insure that the Eastman membrane HT-OO could be used as a nonrejecting film, we determined the relationship between flux and rejection [Equation (9)] experimentally. The results are given in Figure 5, which shows that for flux less than 30 g.p.d./sq.ft., salt rejection was less than 3%. The data of Figure 5 are consistent with a -1 slope, which is in agreement with Equation (9). For such low salt rejection, the coupling coefficient is probably close to unity. Therefore, in order for Equation (7) to reduce to Equation (9), the flow parameter σ must be less than unity.

The use of Equation (14) requires a knowledge of the coefficient for ordinary diffusion in the nonrejecting layer. The diffusivity in porous media is a strong function of porosity (*18* to *23*). When the ratio of the effective diffusivity in a medium with porosity ϵ to the diffusivity in pure solvent is represented by a power law

$$\frac{\mathcal{D}_g}{\mathcal{D}} = \epsilon^n \qquad (23)$$

the value of n is generally constant for diffusion in a given type of porous medium. However, the value of n has been reported (*18, 20, 23, 24*) to be from 1 to 4.6 for various systems and we chose to determine the diffusion coefficients experimentally.

Self-diffusion coefficients for 0.1 *M* NaCl diffusing through the two types of porous films were measured at 25°C. by the radiometric porous-frit method. The experimental apparatus was that used in previous studies (*23, 25, 26*) which should be consulted for details of the technique.

Briefly, the porous films were secured in a platinum screen envelope and saturated with a 0.1 *M* NaCl solution containing a radioactive sodium tracer. The film was then placed in a flow cell, in which 0.1 *M* NaCl circulated past the frit. The decrease in tracer concentration in the film was measured as a function of time, from which data the diffusion coefficient was determined using the equation

TABLE 1. PROPERTIES OF FILMS USED AS NONREJECTING LAYERS

Film	Thickness, μ	Porosity,* %	$\mathcal{D}_g$,† (sq.cm./sec. $\times 10^5$)
Eastman HT-00	100	70	0.58
0.1 μ Millipore	117	74	0.60

* Manufacturer's specification.
† 0.1 *M* NaCl at 25°C.

$$\mathcal{D}_g = 0.0702\,\delta_g^2/t_{1/2} \qquad (24)$$

Tracer half-times were determined at different flow rates; the half-time associated with the membrane alone (that is, no hydrodynamic boundary layer) was determined by extrapolation to infinite velocity on a plot of $t_{1/2}$ versus (velocity)$^{-0.8}$. The effective diffusion coefficients are given in Table 1 along with other properties of the films. In the subsequent sections of the paper the diffusion coefficient was corrected for temperature assuming the diffusion coefficient was inversely proportional to viscosity.

EXPERIMENTAL RESULTS

Variation of Velocity and Layer Thickness

The effect of permeable layer thickness and axial velocity on observed rejection is given by Equation (13). Since there is only a small variation in flux v in turbulent flow (*5, 14*), the term $v\,\delta_g/\mathcal{D}_g$ in Equation (13) is substantially constant for a given layer thickness. Consequently a plot of $\ln(1 - R_{obs}/R_{obs})$ versus $v/u^{3/4}$ should be a straight line with an intercept at $v/u^{3/4} = 0$ equal to

$$\ln\left[\frac{1-R_{obs}}{R_{obs}}\right]_{u=\infty} = \ln\left[\frac{1-R}{R}\right] + \frac{v\,\delta_g}{\mathcal{D}_g} \qquad (25)$$

and with a slope independent of layer thickness.

Using Aerojet-General membranes, both uncovered and covered with two layers (200 μ thick) of Eastman HT-00, we varied the velocity from 2.3 to 22 ft./sec. ($5{,}900 \leq N_{Re} \leq 62{,}000$), holding the pressure constant at 800 lb./sq.in. gauge; the temperature was ~31°C. Feed was demineralized water spiked with 0.08 *M* NaCl. In a similar run with Aerojet-General membranes covered with a single layer of Eastman HT-00 (100 μ thick) axial velocity was varied from 3.4 to 24 ft./sec. with the pressure held constant at 780 lb./sq.in. gauge. Feed was demineralized water spiked with 0.10 *M* NaCl; the temperature was

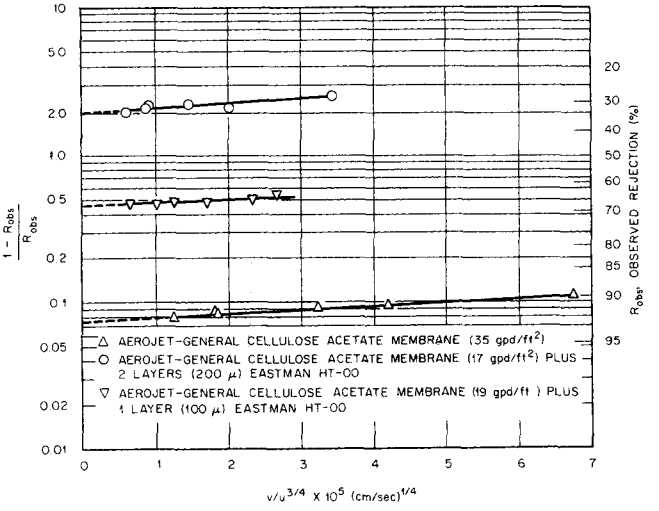

Fig. 6. Variation in observed rejection during velocity excursion using cellulose acetate membranes with and without permeable films (~800 lb./sq.in. gauge; demineralized water spiked with ~0.1 *M* NaCl).

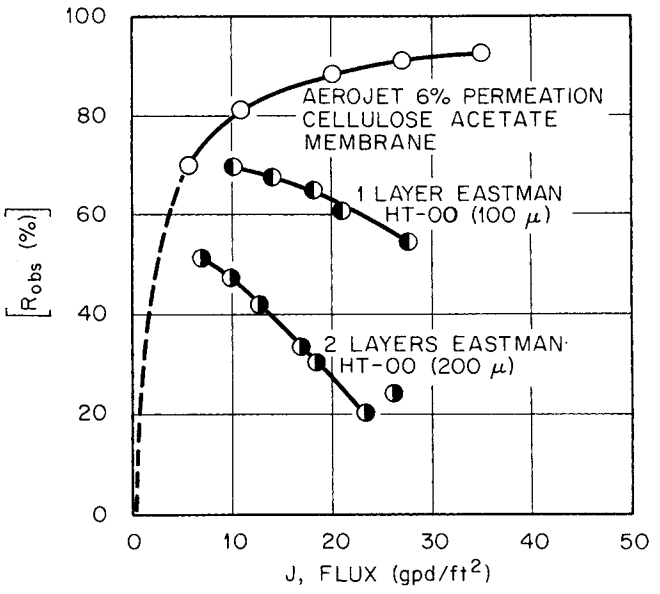

Fig. 7. Variation in observed rejection with flux and thickness of a permeable film on the high pressure side of an Aerojet-General cellulose acetate membrane (24 ft./sec.; 30°C.; 0.1 M NaCl + demineralized water feed).

~30°C.

The results of these two runs are shown in Figure 6 as $\ln(1 - R_{obs})/R_{obs}$ versus $v/u^{3/4}$. The results for a single layer covering the membrane were obtained using a membrane with an intrinsic rejection of 91.8% (compared with 93.1% for the other two sets of points shown on Figure 6). Therefore the single layer results were corrected for this small difference in rejection using Equation (13). Extrapolation of the curves to infinite axial velocity gives intrinsic rejections of $R = 93.1\%$ for the membrane alone, 68.5% for the membrane plus one layer of HT-00, and 34% for the membrane plus two layers of HT-00. [Note that for the uncovered membrane the value of $(1 - R_{obs})/R_{obs}$ at $v/u^{3/4} = 1.25 \times 10^{-5}$ (cm./sec.)$^{1/4}$ ($u = 22$ ft./sec.) is 0.079. This is only ~7% greater than the value $(1 - R)/R = 0.074$ obtained by extrapolation of these results to infinite circulation velocity. This is consistent with our previous statement that, for a plot such as Figure 4, the error in plotting $(1 - R_{obs})/R_{obs}$ at 24 ft./sec. instead of $(1 - R)/R$ was less than 10%.]

Variation of Flux

With an Aerojet-General membrane covered by one layer (100 μ thick) of the HT-00 film, flux and observed rejection were measured at system pressures of 400, 600, 800, and 1,300 lb./sq.in. gauge and at an axial velocity of 24 ft./sec. Feed was demineralized water spiked with 0.11 *M* NaCl; temperature was ~26°C. With two layers (200 μ thick) of HT-00 on the Aerojet-General membrane, flux and observed rejection were measured while the pressure was varied from 200 to 1,300 lb./sq.in. gauge at an axial velocity of 24 ft./sec. Feed was demineralized water spiked with 0.09 *M* NaCl; the temperature was ~30°C.

The results of these two pressure excursions at 24 ft./sec. axial velocity are shown in Figure 7 where rejection is plotted as a function of flux. Also shown are the results of Figure 4 for the uncovered Aerojet-General membrane. For the membranes covered with nonrejecting films, R_{obs} decreases with increasing flux and layer thickness as qualitatively predicted by Equation (14). The results given in Figure 7 clearly show that doubling the flux and doubling the layer thickness affect observed rejection to different extents. This is because the intrinsic rejection is a function of flux over the range of flux studied, as predicted in Equation (9) and shown in Figure 4. The effect of the nonrejecting layers is also demonstrated by plotting the results of Figure 7 as log $(1 - R_{obs}/R_{obs})$ versus log (J). The results for the uncovered membrane have slope of -1. However, the results for membranes covered with nonrejecting layers have a positive slope (Figure 8).

Pressure excursions were also performed with Millipore filters covering Eastman RO-97 cellulose acetate membranes. System pressure was varied from 200 to 1,300 lb./sq. in. gauge with the axial velocity again at 24 ft./sec. Feed was demineralized water spiked with 0.09 M NaCl; the temperature was ~30°C.

Correlation of Results

The results of all pressure excursion experiments with different permeable membranes, different fluxes, and different film thicknesses are given in Figure 9 with coordinates suggested by Equation (14), $[\{(1 - R_{obs})/R_{obs}\}/\{(1 - R)/R\}]$ versus $(v\ \delta_g/\mathcal{D}_g)$. The intrinsic rejection was determined from Figure 4 for a given value of flux v. Figure 9 shows that the separation of the data according to layer thickness, seen in Figures 7 and 8, has been eliminated and data for one and two thicknesses each of two nonrejecting films on different cellulose acetate membranes reduce to a single curve. The solid line was calculated from Equation (14) and shows good agreement of theory with the experimental results.

DISCUSSION

With the present equipment, fully developed turbulent flow occurred for Reynolds numbers greater than 10^4, or velocities greater than 3.5 ft./sec. At a flux of ~28 g.p.d./sq.ft., the ratio of $(1 - R_{obs})/R_{obs}/(1 - R)/R$ for an uncovered membrane decreased from 1.15 to 1.03 as the velocity was increased from 3.5 to 24 ft./sec. However, when a 100-μ thick permeable layer with ~70% voids covered the same membrane, the ratio $(1 - R_{obs})/R_{obs}/(1 - R)/(R)$ was 8.5 at the same flux and an axial velocity of 24 ft./sec. In other words, permeable layers covering salt rejecting membranes may have a more pronounced

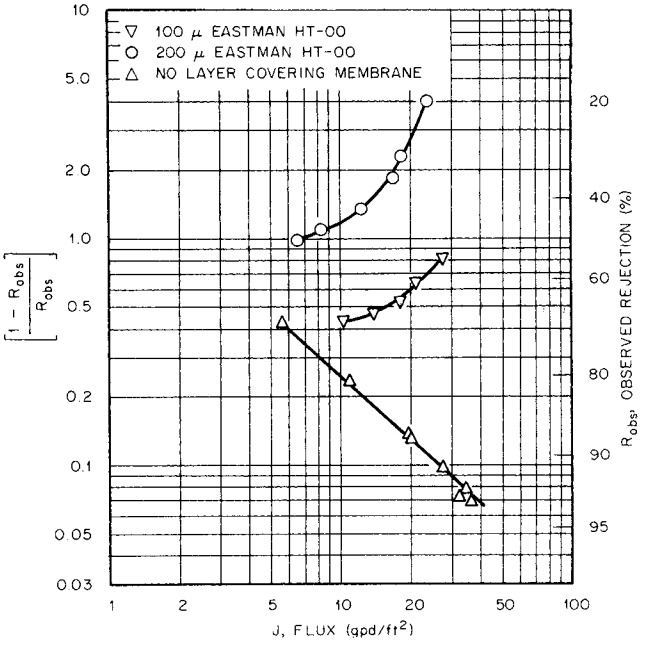

Fig. 8. Variation in observed rejection with flux through Aerojet-General 6% permeation cellulose acetate membrane covered with various thicknesses of a permeable film (24 ft./sec; ~30°C.; ~0.1 M NaCl in demineralized water).

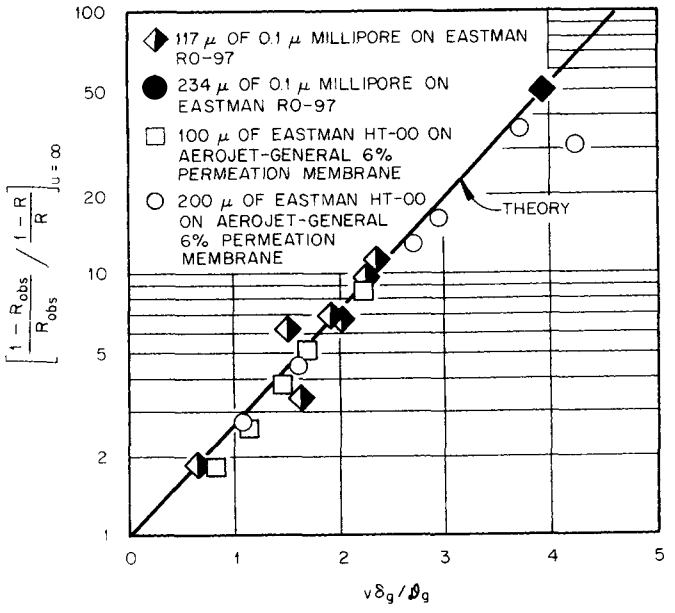

Fig. 9. Effect of placing various permeable films on the high pressure side of cellulose acetate membranes [0.1 M NaCl in demineralized water; 30°C.; theory line given by Equation (14) in text].

effect on observed rejection and hence on product water quality than does axial velocity in turbulent flow. In the present example, the permeable layer thickness would have to be reduced to less than 10 μ to achieve a value of $[(1 - R_{obs})/R_{obs}/(1 - R)/R] = 1.15$.

As shown by Equation (14) and Figure 6, once a membrane is covered by a permeable film or fouling layer, there is little effect of axial velocity on the rejection characteristics, provided the film maintains its integrity as the velocity is varied.

ACKNOWLEDGMENT

The authors acknowledge the support and suggestions of Kurt A. Kraus, the assistance of P. H. Hayes in performing the experimental measurements, and H. O. Phillips for providing equipment and guidance for the diffusion coefficient measurements. This paper is based on a portion of the Ph.D. dissertation of John D. Sheppard in partial fulfillment of the requirements of the University of Tennessee.

The research on which this paper is based was sponsored by the Office of Saline Water, U.S. Department of the Interior, under the Union Carbide Corporation contract with the U.S. Atomic Energy Commission.

NOTATION

c = salt concentration (M)
c_α = salt concentration at the membrane-feed stream interface (M)
c_ω = salt concentration in the product stream (M)
c_i = salt concentration at the film-feed stream interface (M)
c_t = salt concentration in the feed stream (M)
$\mathcal{D}$ = salt diffusion coefficient in water, sq.cm./sec.
$\mathcal{D}_2^*$ = salt diffusion coefficient in membrane, sq.cm./sec.
$\mathcal{D}_g$ = equivalent salt diffusion coefficient in a porous medium, sq.cm./sec.
J = product transmission rate, g.p.d./sq.ft.
k = constant in Equation (6), dimensionless
l = membrane (active layer) thickness
m = salt concentration (m)
N_{Re} = Reynolds number, dimensionless
N_{Sc} = Schmidt number, dimensionless
P = pressure, atm.
$\mathcal{P}$ = permeability, g.p.d./(sq.ft.)(atm.)
R = intrinsic rejection, dimensionless
R_{obs} = observed rejection, dimensionless
$\mathcal{R}$ = gas constant
$t_{1/2}$ = tracer concentration half-time, sec.
T = absolute temperature, °K.
u = axial velocity, cm./sec.
v = transverse velocity, cm./sec.
y = dimension normal to the membrane surface, cm.

Greek Letters

δ_g = nonrejecting layer thickness, cm.
δ_{BL} = boundary-layer thickness, cm.
δ_t = value of y at $c = c_t$, cm.
ϵ = porosity, dimensionless
ν = ionic species per molecule, dimensionless
π = osmotic pressure, atm.
φ = osmotic coefficient, dimensionless
ψ = concentration polarization, dimensionless
ψ_g = concentration polarization in the nonrejecting layer, dimensionless
ψ_{BL} = concentration polarization in the concentration boundary layer, dimensionless

LITERATURE CITED

1. Suddak, R. G., *OSW R&D Rept. No. 453* (1969).
2. Aerojet-General Corp., *OSW R&D Rept. No. 213* (1966).
3. Loeb, S., and J. S. Johnson, *UCLA Dept. Eng. Rept. No. 66-61* (1966).
4. McCutchan, J. W., and J. S. Johnson, *J. Am. Water Works Assoc.*, **62**, 346 (1970).
5. Sheppard, J. D., and D. G. Thomas, *Appl. Polym. Symp.*, No. 13, 121-138 (1970).
6. Vos, K. D., F. Burris, and R. L. Riley, *J. Appl. Polymer Sci.*, **10**, 825 (1966).
7. Johnson, J. S., L. Dresner, and K. A. Kraus in "Principles of Desalination," K. S. Spiegler, Ed., Chap. 8, Academic Press, New York (1966).
8. Robinson, R. F., and R. H. Stokes, "Electrolytic Solutions," 2nd edit., Butterworth, London (1965).
9. Sherwood, T. K., P. L. T. Brian, R. E. Fisher, and L. Dresner, *Ind. Eng. Chem. Fundamentals*, **4**, 113 (1965).
10. Brian, P. L. T., "Proceedings of the First International Symposium on Water Desalination," Vol. 1, p. 349 (1965).
11. ———, in "Desalination by Reverse Osmosis," U. Merten, Ed., Chap. 5, Massachusetts Inst. Technol. Press (1966).
12. Shor, A. J., K. A. Kraus, J. S. Johnson, and W. T. Smith, *Ind. Eng. Chem. Fundamentals*, **7**, 44 (1968).
13. Kraus, K. A., A. J. Shor, and J. S. Johnson, *Desalination*, **2**, 24-266 (1967).
14. Sheppard, J. D., and D. G. Thomas, *ibid.*, **8**, 1-12 (1970).
15. Thomas, D. G., and J. S. Watson, *Ind. Eng. Chem. Process Design Develop.*, **1**, 97 (July 1968).
16. Mixon, W. R., M.S. thesis, Univ. of Tennessee, Knoxville (1969).
17. Raridon, R. J., L. Dresner, and K. A. Kraus, *Desalination*, **1**, 210 (1966).
18. Satterfield, C. N., and T. K. Sherwood, "The Role of Diffusion in Catalysis," Addison-Wesley (1963).
19. Hoogschagen, J., *Ind. Eng. Chem. Design Process Develop.* **44**, 906 (1955).
20. Curie, J. A., *Brit. J. Appl. Phys.*, **11**, 314 (1960).
21. Piret, E. L., R. A. Ebel, C. T. Kiang, and W. P. Armstrong, *Chem. Eng. Progr.*, **47**, 405 (1951).
22. *Ibid.*, 628.
23. Phillips, H. O., A. E. Marcinkowsky, and K. A. Kraus, paper presented at AIChE Atlantic City meeting (Sept. 1965).
24. Wang, J. H., *J. Am. Chem. Soc.*, **76**, 4755 (1954).
25. Marcinkowsky, A. E., S. Nelson, and K. A. Kraus, *J. Phys. Chem.*, **69**, 303 (1965).
26. Marcinkowsky, A. E., H. O. Phillips, and K. A. Kraus, *ibid.*, **72**, 120 (1968).
27. Michaels, A. S., *Chem. Eng. Progr.*, **64** (12), 31 (1968).

Manuscript received April 22, 1970; revision received June 23, 1970; paper accepted June 29, 1970.